NRC Publications Archive
Archives des publications du CNRC

Modulation of polycaprolactone composite properties through incorporation of mixed phosphate glass formulations

Shah Mohammadi, Maziar; Ahmed, Ifty; Marelli, Benedetto; Rudd, Christopher; Bureau, Martin N.; Nazhat, Showan N.

This publication could be one of several versions: author’s original, accepted manuscript or the publisher’s version. / La version de cette publication peut être l’une des suivantes : la version prépublication de l’auteur, la version acceptée du manuscrit ou la version de l’éditeur.
For the publisher’s version, please access the DOI link below./ Pour consulter la version de l’éditeur, utilisez le lien DOI ci-dessous.

Publisher’s version / Version de l'éditeur:
https://doi.org/10.1016/j.actbio.2010.03.002
Acta Biomaterialia, 6, 8, 2010

NRC Publications Record / Notice d'Archives des publications de CNRC:
https://nrc-publications.canada.ca/eng/view/object/?id=62aa93b9-52da-4cc1-87af-efce2f84a667
https://publications-cnrc.canada.ca/fra/voir/objet/?id=62aa93b9-52da-4cc1-87af-efce2f84a667

Access and use of this website and the material on it are subject to the Terms and Conditions set forth at
https://nrc-publications.canada.ca/eng/copyright
READ THESE TERMS AND CONDITIONS CAREFULLY BEFORE USING THIS WEBSITE.

L’accès à ce site Web et l’utilisation de son contenu sont assujettis aux conditions présentées dans le site
https://publications-cnrc.canada.ca/fra/droits
LISEZ CES CONDITIONS ATTENTIVEMENT AVANT D’UTILISER CE SITE WEB.

Questions? Contact the NRC Publications Archive team at PublicationsArchive-ArchivesPublications@nrc-cnrc.gc.ca. If you wish to email the authors directly, please see the first page of the publication for their contact information.

Vous avez des questions? Nous pouvons vous aider. Pour communiquer directement avec un auteur, consultez la première page de la revue dans laquelle son article a été publié afin de trouver ses coordonnées. Si vous n’arrivez pas à les repérer, communiquez avec nous à PublicationsArchive-ArchivesPublications@nrc-cnrc.gc.ca.

National Research Council Canada
Conseil national de recherches Canada

Text only

Modulation of polycaprolactone composite properties through incorporation of mixed phosphate glass formulations

Maziar Shah Mohammadi[1], Ifty Ahmed[2], Benedetto Marelli[1], Christopher Rudd[2], Martin N Bureau[3], Showan N Nazhat[1*]

[1] Department of Mining and Materials Engineering, McGill University, Montreal, QC, Canada.

[2] Faculty of Engineering, Division of Materials, Mechanics and Structures, University of Nottingham, U.K.

[3] Industrial Materials Institute, National Research Council Canada, QC, Canada

Keywords: Phosphate-based glass particles, polycaprolactone, biodegradable composites, dissolution, bioactivity

***corresponding author** showan.nazhat@mcgill.ca

Acknowledgements: This work was funded by the Canadian Natural Sciences and Engineering Research Council, Le Fonds québécois de la recherche sur la nature et les technologies, Hatch Faculty Fellowship and Canadian Foundation for Innovation: Leaders Opportunity Fund. Funding for Maziar Shah Mohammadi and Benedetto Marelli was also partly supported by McGill Engineering Doctoral Awards and the Werner Group, respectively. The authors thank Monique Riendeau, Saurav Mohapatra, Christoph Stahli, Jason Betram, and Hye-Lim Choi for their assistance in this work. Milan Maric's group in Department of Chemical Engineering, McGill University is thanked for GPC analysis. The authors also thank the Composites Research Group at the University of Nottingham for their support. Showan Nazhat is a member of the Centre for Bone and Periodontal Research.

Abstract

Phosphate-based glasses (PGs) and their composites are of interest as bone repair and tissue engineering scaffolds due to the totally degradable nature of the materials. This study investigated the effect of Si and Fe on the properties of PG particulate-filled polycaprolactone (PCL) matrix composites. Two glass compositions were investigated (in mol%): 50 P_2O_5, 40 CaO and 10 SiO_2 or Fe_2O_3 (Si_{10} and Fe_{10} respectively). All composites contained 40 vol% particulate filler, either of Si_{10}, Fe_{10}, or a blend ($40Si_{10}/0Fe_{10}$, $30Si_{10}/10Fe_{10}$, $20Si_{10}/20Fe_{10}$, $10Si_{10}/30Fe_{10}$, $0Si_{10}/40Fe_{10}$). Ion release, weight loss and composite mechanical properties were characterized as a function of time in deionised water (DW) and phosphate buffered saline (PBS), respectively. The potential for calcium phosphate deposition was assessed in simulated body fluid (SBF).

Calcium and phosphate ions release in DW increased in tandem with the rate of composite weight loss, which increased with Si_{10} content. A Si_{10} content dependent rate of pH reduction was observed in DW. At day 56, PG in $40Si_{10}/0Fe_{10}$ composite completely dissolved, whereas 67% of the $0Si_{10}/40Fe_{10}$ remained. The initial flexural strength of $40Si_{10}/0Fe_{10}$ composites was significantly lower when compared to the other materials. An increase in Si_{10} content led to an increase in Young's modulus and a concomitant decrease in flexural strain. It was found that the PCL molecular weight (M_w) was significantly decreased with an increase in Si_{10} content. FTIR analysis showed that Si incorporation into PG led to their reaction with the PCL ester bonds resulting in a reduction in PCL M_w when processed at elevated temperatures. Changes in mechanical properties with time in PBS were glass blend dependent and a more rapid rate of reduction was observed in Si_{10} dominant composites. At day 28 in SBF, surface deposited

brushite was formed in $20Si_{10}/20Fe_{10}$ PG containing composites. Therefore the properties of PCL-PG composites could be tailored by controlling the phosphate glass blend composition.

1. Introduction

Composites are an attractive approach as biomaterials since advantageous properties of different materials can be combined to satisfy the required mechanical and physiological demands of the host tissue [1, 2]. Composites based on biodegradable polymers and bioactive ceramics have been considered for bone tissue engineering, reconstruction and repair [3-5]. Incorporation of ceramics and glasses into the polymer matrix should improve not only the mechanical properties of the material, but also its bioactivity and biological behaviour [6]. Therefore, bioactive fillers of calcium phosphates have been incorporated in degradable polymers [7-12]. Since the composition of the filler, its content and solubility are parameters that can influence composite properties, the tailoring of such properties is paramount. However, not all calcium phosphate materials are necessarily ideal. For example, hydroxyapatite (HA) or bioactive silicate-based glasses do not reflect the required dissolution properties [13]. Therefore, producing a biodegradable composite material with controllable dissolution criteria is essential in bone repair and regeneration. For this purpose, phosphate-based glasses (PGs) may be a potential alternative as the inorganic phase of biodegradable composites [14, 15].

PGs provide a diverse range of solubility, which can be predicted and controlled by altering their composition [16-19]. Numerous binary, ternary and quaternary PGs have been developed [16-25]. A ternary glass system based on $45P_2O_5$-XCaO-(55-X)NaO_2, where X was between 8 and 40 mol%, was developed by Franks *et al.* [18]. An inverse relationship between CaO content and the solubility was observed, which was linear over time for glasses containing up to 20 mol% CaO. It was suggested that Ca^{2+} and its interaction with the glass network were the dominant factors of dissolution. In high CaO content PGs, an ion exchange process and a gradual breakdown of the glass network were two suggested processes responsible for dissolution. Salih *et al.* [26] investigated the potential of this glass system for bone regeneration and suggested that, at higher CaO content, greater amounts of Ca^{2+} are released with lower dissolution rates, which has an essential role in cell activation mechanisms affecting cell growth. However, a sharp change in pH associated with high release rates of Na^+ and PO_4^{3-} has an adverse effect on cells in highly soluble glasses and unfavourable cellular responses associated with glasses of high Na^+ content. Ahmed *et al.* [27] partially substituted Na_2O by Fe_2O_3 in PG to provide more control over solubility. Fe_2O_3 addition up to 5 mol% resulted in a decrease in solubility by one order of magnitude and an increase in the glass transition temperature due to the formation of more hydration resistant P-O-Fe bonds [28]. This formulation also allowed the adhesion and proliferation of myoblasts *in vitro*. Incorporation of SiO_2 into PG, on the other hand, has been shown to increase their solubility. PG with the composition of $50P_2O_5$-30CaO-(15-X)Na_2O-$5Fe_2O_3$-$XSiO_2$ was investigated by Patel and Knowles [16]. The substitution of SiO_2 up to 3 mol% resulted in glasses with a linear solubility behaviour reaching 20% weight loss at day 7, whereas the addition of 5 mol% led to glasses with a non-linear solubility behaviour reaching 60% weight loss at day 4.

The versatility of PG properties may be translated to a composite system by incorporation into a degradable polymer. However, this has largely depended on the glass composition, which has tended to be based on one type of filler [6-9]. Therefore, in this study, PG particles ($50P_2O_5$-40CaO-10X) where X is either Fe_2O_3 or SiO_2 were incorporated into polycaprolactone (PCL) to serve as a degradable composite biomaterial for potential applications in bone repair and regeneration. It is hypothesised that PCL incorporated PG particulate blends of different formulations will tailor the composite properties. Changes in structural and mechanical properties in deionised water and phosphate buffered saline, and the potential for a calcium phosphate deposition by conditioning in simulated body fluid were investigated.

2. Experimental

2.1. Materials

2.1.1. Phosphate glass particulate (PGP) production

Two melt derived glass compositions were prepared using P_2O_5, $CaHPO_4$, Fe_2O_3, and SiO_2 (Sigma Aldrich, UK) as starting materials. The precursors were mixed and placed into a Pt/5%Au crucible (Birmingham Metal Company, UK), and heated to 400 °C for half an hour to remove moisture. They were then melted at 1150 °C for 90 min, poured onto a steel plate and quench cooled to room temperature. Table 1 lists the glass compositions and codes. Bulk glass was ground using agate media in a vibratory cup mill (KHD Humboldt Wedag AG MN 954/2, Christison Scientific Equipment Ltd, Gateshead, UK) for 6 min and sieved for 20 min using three-sieve stacks of 105, 75, and 53 μm. Approximately 67% passed through the 53 μm sieve in the allocated grind time.

2.1.2 PCL-PG composite production

PCL-PGP composites were prepared by first dissolving PCL (average Mw ~65,000, Sigma Aldrich, U.K.) in chloroform (Laboratory grade, Fisher Scientific) at 7% (v/v) followed by addition of appropriate amounts of PGP and the solution was allowed to mix for 20 min. The solution was then ultrasonicated (Precision Ultrasonic Cleaner from Ultrawave Limited, Cardiff, UK) for 1 min, and poured into a 13.5 cm-diameter petri dish. Films were then prepared by solvent casting at room temperature for two days. Composites of approximately 1.6 mm thickness were produced from five films placed in a metal shim, and heat-pressed (Daniels Down-stroke Press, UK) at 100 °C. The films were heated for 30 min and pressed for 30 min at

38 bar, after which they were immediately cooled in a second press (Daniels Up-stroke Press, UK) at room temperature for 30 min at the same pressure. Table 2 lists composite compositions and codes. Composites containing 40 vol% PG particles, either of Si_{10}, Fe_{10}, or a blend ($40Si_{10}/0Fe_{10}$, $30Si_{10}/10Fe_{10}$, $20Si_{10}/20Fe_{10}$, $10Si_{10}/30Fe_{10}$, $0Si_{10}/40Fe_{10}$), were prepared.

Neat PCL plaques (also 1.6 mm thick) was also produced by melt pressing PCL for 30 min at 38 bar and cooling in the cold press at room temperature for a further 30 min at 38 bar.

2.2. Characterisation of the PCL-PGP composites

2.2.1. Ageing in deionised water (DW)

PCL-PGP composites were aged in DW for up to 56 days by placing 10 x 10 x 1.6 mm^3 specimens (n=3) into vials containing 25 ml of ultra-pure deionised water (18.2 MΩ cm resistivity) and incubating at 37 °C. Ion release, composite weight, and pH of the ageing environment were measured at 14 different time points 0, 2, 4, 8, 24, 48, 96, 168, 336, 504, 672, 840, 1008, and 1344 hours.

Anion and cation release through PGP dissolution were measured using ion chromatography (IC) and atomic absorption (AA), respectively. IC (Dionex, DX-100 Ion chromatograph) was used in order to measure phosphate anion (PO_4^{3-}) release. An Ionpac^R AS14 anion exchange column was used to elute the polyphosphates. An eluent of 3.5 mM Na_2CO_3/0.1 mM $NaHCO_3$ was used with a flow rate of 0.1 ml/min. The sample run time was 15 min. Sodium phosphate tribasic (Na_3PO_4) (Sigma, Canada) was used to prepare standard solutions. A 1000 ppm working solution was prepared from which serially diluted 10, 20, and 50 ppm standard solutions were obtained. AA (Varian AA240FS) was used to investigate the release of Ca^{2+}, Fe^{3+}, and Si^{4+} cations. The instrument was calibrated using certified AA standard solutions.

The weight change of the composites was investigated by removing the specimens from DW, blot drying, weighing and replacing in fresh deionised water. Weight loss was measured in terms of percentage of original weight. The final dry weight at day 56 was measured by first incubating the specimens at 37 °C until an equilibrium weight was reached. The pH of the deionised water was also measured using a pH meter (Accumet Excel 20, Fisher) at each time point.

2.2.2. Morphological investigations using scanning electron microscopy (SEM)

SEM (JEOL JSM 6100, Tokyo, Japan and Hitachi S-4700) was used to investigate the morphology of the composites before and after ageing in DW. Both secondary electron (SE) and back scattered electron (BSE) modes with accelerating voltages of 1 and 10 kV, were used respectively. The samples were cryo-fractured and the resulting fracture surfaces were coated with gold or palladium using sputter coaters.

2.2.3. Composite initial mechanical properties and as a function of time in PBS

Three-point bend flexural mechanical analysis was used to measure the mechanical properties of the composites. The effect of PG formulation on composite mechanical properties was investigated through changes in flexural strength, Young's modulus, and strain at maximum stress. Tests were performed on initially produced and PBS (Sigma Aldrich, CA) aged specimens stored at 37 °C and tested at days 7 and 28. Weight loss upon PBS ageing was monitored prior to mechanical testing, by first drying the specimens. At least three repeat specimens were tested with a cross-head speed of 1 mm/min using a 1 kN load cell and according to ASTM D 790-95a:1996 (aspect ratio > 16) in an Instron mechanical testing instrument 5582 (Instron Ltd).

2.2.4. Molecular weight determination

Gel permeation chromatography (Water Breeze) was used to investigate the molecular weight (M_w) of PCL both after composite fabrication and at day 56 in DW. The GPC was equipped with both ultraviolet (UV 2487) and differential refractive index (RI 2410) detectors and three Water Styragel HR columns (HR1 with molecular weight measurement in the range of 102 -5x10^3 g/mol, HR2 with molecular weight measurement range of 5x10^2 -2x10^4 g/mol, and HR4 with molecular weight measurement range of 5x10^3 - 6x10^5 g/mol and a guard column. The columns were kept at 40 °C. Tetrahydrofuran (THF) flowing at a rate of 0.3 ml/min was used as the mobile phase. Each sample dissolved in THF was filtered through a 0.2 μm syringe filter (Anotop25, Fisher) to remove PGP prior to injection into the module.

2.2.5. Fourier transform infrared spectroscopy (FTIR)

FTIR spectroscopy was used to investigate the structural changes in the PCL matrix due to its potential interactions with PGP when processed at high temperature. Polymer and composite films (Table 2) were first prepared through solvent casting (low temperature) and then heated while spectra were collected. Composite films of approximately 75 μm thickness were prepared by first dissolving PCL pellets of 1 g in 23.5 ml chloroform and the appropriate amounts of PGP were added to the solution and ultrasonicated for 5 min.

FTIR spectroscopy was carried out using a Perkin Elmer Spotlight 400 FTIR microscope connected to a Spectrum 400 infrared beam source (Perkin Elmer Instruments, Canada) on disk-shaped specimens (nominal diameter of 13 mm) mounted on a KBr disk (N9302615, Perkin Elmer). The microscope was used in transmission mode in the mid infrared region (4000-650 cm^{-1}) with a resolution of 8 cm^{-1} and number of scans of 8. A heating chamber was used (BriskONE, BriskHeat Corp.) to increase the temperature from 25 to 60°C at 25°C/min, hold for 10 min, then increase to 100°C and hold for 60 min. The system was then cooled down to room temperature for 30 min. The Spectrum Timebase v2.0 software (Perkin Elmer) was set to record the spectra every 20 s. Since the film was thin enough for the Beer-Lambert law to be valid, the changes in the IR spectrum during the thermal process are an indication of chemical modifications. The kinetics of the PCL degradation at 100°C was investigated as proposed by Blaker *et al.* [29].

2.2.6. Conditioning in simulated body fluid (SBF)

Three repeat specimens (10 x 10 x 1.6 mm^3) of each composite were placed into vials containing 60 ml of SBF and incubated at 37 °C. The SBF solution was prepared according to Kokubo *et al* [30] and replaced every 3 days. The containers were removed from the incubator at days 7, 14, and 28. Precipitates formed on the surface of the composites were analysed using SEM (Hitachi S-4700) and X-Ray powder diffraction (XRD, Bruker D8). Composite weight change and SBF pH were also measured at regular time intervals.

3. Results

3.1. Ageing in DW

3.1.1. Anion release (PO_4^{3-})

Figure 1-a shows the PO_4^{3-} ion release measurements as a function of time. There was an increase in PO_4^{3-} ion released with an increase in Si_{10} glass content in the composites. A prompt release of PO_4^{3-} was observed for PCL-PGP 1 in the first 24 hours. The rate of PO_4^{3-} ion release decreased considerably by substituting Si_{10} with Fe_{10}; however, there was a continual release of PO_4^{3-} ion over time for PCL-PGP 2-5.

3.1.2. Cation release (Ca^{2+}, Fe^{3+}, Si^{4+})

Figure 1-b shows the Ca^{2+} ion release as a function of time. By increasing the Si_{10} content in the composites, a higher rate of Ca^{2+} ion was released. As expected the highest Si^{4+} ion release (Figure 1-c) was observed for PCL-PGP 1. The other composites showed similar release profiles up to approximately the 200 hour time point, after which a continual release of Si^{4+} was observed

for the duration of the study. Interestingly, more Fe^{3+} ions were released as the Si_{10} content increased (Figure 1-d).

3.1.3. Weight loss measurements

The weight change of the composites in DW are shown in Figure 1-e in terms of the percentage of original weight versus time. A prompt weight loss was observed for both PCL-PGP 1 and 2 (up to 168 h) which was followed by a much slower rate of weight loss, reaching approximately 42% in PCL-PGP 1. PCL-PGP 3 showed a similar profile, however, with a lower rate of weight loss that was continual up to day 56, whilst PCL-PGP 4 displayed an even slower rate of weight loss, reaching 17%. PCL-PGP 5 on the other hand showed a weight gain at day 4, which was followed by a slow and continual weight loss up to day 56. Neat PCL demonstrated no weight loss in the entire ageing period.

Table 3 gives the final dry weight of the composites at day 56. Data revealed that there was no residual glass left in PCL-PGP 1 and 2. The residual glass in PCL-PGP 3, 4, and 5 were approximately 12, 44, and 67%, respectively, demonstrating intermediate dissolution levels based on the percentages of Si_{10} and Fe_{10}.

3.1.4 pH change

The associated change in pH of DW was measured at each time point for all materials and is shown in Figure 1-f. The pH values of PCL-PGP 1 dropped significantly at early time points and then increased rapidly to the initial pH value, indicating that all the glass had dissolved. All other composites demonstrated similar behaviours, with the exception of PCL-PGP 5 which showed a delayed decrease in pH. Overall a slower rate of pH reduction was seen with an increase in Fe_{10} content. The pH of neat PCL remained relatively constant.

3.2. Morphological investigations

Figure 2-a shows a SEM micrograph of an as-prepared PCL-PGP 3 composite as an example of glass particle distribution within the polymer matrix. Figure 2-b revealed that at day 56 in DW, both glass particles and pores were present in this composite. Porosity was thus attributed to the rapidly dissolving Si_{10} glass particles as EDS analysis revealed that the remaining PGP were from glass code Fe_{10} (data not shown). In contrast, no glass particles were observed in PCL-PGP 1 at day 56 (Figure 2-c). These images corroborate with the weight loss data given in Table 3.

3.3. Mechanical property changes in PBS

Figure 3-a shows the weight loss of the composites aged in PBS and demonstrates a similar weight loss effect seen in DW. Final dry weight of PCL-PGP 1 confirmed that all the glass particles had dissolved. In contrast, PCL-PGP 5 resulted in a 7% weight loss at day 28, and the other composites gave intermediate levels. Initial mechanical analysis (Figure 3 b-d) of the composites revealed that the flexural strength of PCL-PGP 1 was significantly lower ($p<0.05$) as compared to the remaining composites tested. PGP incorporation resulted in a significant increase in Young's modulus which was composition dependent and tended to increase with Si_{10} content. The modulus values ranged from 0.3 ± 0.03 to 1.5 ± 0.20 to 3 ± 0.78 GPa for PCL, PCL-PGP 5, and PCL-PGP 1 respectively. In parallel, the strain at maximum stress decreased significantly ($p<0.05$) by increasing the Si_{10} content.

The mechanical properties of neat PCL did not change significantly by ageing in PBS, while those of PCL-PGP decreased progressively, with the composites with higher Si_{10} contents demonstrating a more rapid decrease. For example, at day 7 in PBS, while the strength of PCL-PGP 2 and 5 decreased by 85 and 26%, respectively, PCL-PGP 1 properties could not be measured due to their loss of integrity. At day 28 in PBS, the Young's modulus values of PCL-

PGP 2 and 5 decreased by 90 and 28%, respectively while flexural strain underwent a similar significant decrease for these composites (83 and 69% for PCL-PGP 2 and 5, respectively).

3.4. Molecular weight determination

Figure 4-a shows the PCL M_w in the various composites. There was a slight change in PCL M_w in PCL-PGP with no or low Si_{10} content (PCL-PGP 4 or 5). However, PCL M_w significantly decreased in PCL-PGP with higher Si_{10} content. For example, PCL M_w in PCL-PGP 1 decreased 14,000 g/mol. PCL-PGP composites containing both Fe_{10} and Si_{10} showed intermediate M_w values. PCL M_w did not appear to be considerably affected by DW conditioning (Figure 4-a). Polydispersity index of the PCL-PGP also did not vary from that of neat PCL and was not affected by PGP formulation (Figure 4-b).

3.5. FTIR analysis

The fractional absorbance (ϕ) change of the carbonyl peak (1728 cm^{-1}), expressed as ϕ_{1728}, for PCL and PCL-PGP composites is shown in Figure 5-a. PCL-PGP 5 did not show changes when compared to neat PCL. However, there was a considerable increase of ϕ_{1728} for PCL-PGP 1 and 3 with thermal treatment time at 100 °C, indicating that greater changes in the absorbance and fractional absorbance change derivate (dø/dt) were observed at higher Si_{10} content. Therefore, a greater and faster reduction in PCL M_w is expected at higher Si_{10} content. The full spectrum of PCL-PGP 1 before and after thermal treatment is presented in Figure 5-b. There was a reduction in the absorbance of the carbonyl peak and an appearance of the carboxylate peak at 1634 cm^{-1}. While the formation of carboxylate peak was not observed in PCL and PCL-PGP 5, it became more apparent as the Si_{10} content increased as in the case of PCL-PGP 3 and 1 (Figure 5-c). In addition, reduction of the ester absorbance peaks for the asymmetric C-O-C stretching (1240 cm^{-}

^{1}), OC-O stretching (1190 cm^{-1}), and the symmetric C-O-C stretching (1170 cm^{-1}) were observed.

3.6. Conditioning in SBF

The weight change of the composites in SBF are shown in Figure 6-a in terms of the percentage of original weight versus time. A prompt weight loss was seen for PCL-PGP 1 (up to 168h) which remained constant thereafter. PCL-PGP 2 and 3 showed similar behaviours; however, with lower rates of weight loss. A weight gain was observed for PCL-PGP 4 and 5 in the first 48 and 168 h, respectively, followed by a slow rate of continuous weight loss. No weight loss occurred in the neat PCL.

The associated change in pH of the SBF up to 1 week is shown in Figure 6-b. While no change in the pH of SBF medium was observed for neat PCL, the pH of all the composites decreased significantly over time to below 4, the rate of which increased with Si_{10} content.

Figure 7(a-c) shows the images (at days 7, 14 and 28), SEM micrographs (at day 28), EDS as well as XRD patterns (Figure 7 d and e) of the precipitates formed by conditioning in SBF for PCL-PGP 5, 3 and 1. Precipitates were observed on the surfaces of PCL-PGP 2-5. In contrast, no precipitates were found on PCL-PGP 1. EDS analysis confirmed the presence of calcium, phosphorous and oxygen. XRD patterns of PCL-PGP 3 are presented in Figure 7-d, initially, and at days 14, and 28 in SBF. These revealed the formation of brushite (dicalcium phosphate dihydrate, DCPD) precipitates on the surface of the specimens at the latter time point. Figure 7-e compares the XRD patterns of the surface of PCL-PGP 1, 3 and 5 at day 28. While the pattern of PCL-PGP 1 confirmed no brushite formation, the pattern of PCL-PGP 5 suggested a brushite formation potential.

4. Discussion

In this study, particulates of two different PG formulations were incorporated into PCL to potentially produce biodegradable composites of tailored properties for intended applications in bone augmentation and regeneration. While the reinforcement was kept at 40 vol%, the glass composition was varied between two ternary based formulations ranging from a high content of SiO_2 to Fe_2O_3. PG glasses are soluble in aqueous media and upon dissolution can deposit a calcium phosphate (depending on formulation) that may prove to be bioactive. However, to achieve such a goal, the solubility and its effect on composite properties, e.g. structure and mechanics, should be tailored. An ultimate challenge in bone regeneration is the balance between the rate of tissue growth and that of biomaterial degradation. Therefore, by incorporating two different PG formulations with varying solubilities in a degradable polymer matrix, degradable composites with diverse properties could be produced. By doping PG glasses with Fe, the cross-linking between the glass polyphosphate chains are strengthened [21], resulting in higher glass stability (and low solubility). On the other hand, Si can break down the phosphate glass network, leading to higher solubility [16].

Ageing in deionised water showed that the rate of weight loss of the composites was dependent on Si_{10} content. As previously reported by Ahmed *et al* [31], the release rates of PO_4^{3-} and Ca^{2+} ions were in line with the rate of glass dissolution. While Si^{4+} release was dependent on Si_{10}, interestingly, Fe^{3+} showed a similar dependency. The latter can be explained by the rate of ion release dependence on water uptake. With increasing Si_{10} content, the water ingress led to porosity and greater exposure of Fe_{10} glass particle to water leading to their dissolution and an increase of Fe^{3+} release. In the case of PCL-PGP 5, Fe^{3+} release was delayed and coincided with a weight gain in these composites at day 4, indicating the two simultaneous mechanisms: water uptake occurring in the matrix and at the filler-matrix interface with eventual dissolution of PGP resulting in weight loss. Since the solubility of Fe_{10} glasses is relatively low, the weight gain is dominant at early time points. Once the polymer matrix is saturated, weight loss becomes prominent due to glass dissolution [6].

As a consequence of higher solubility, a rapid rate of pH reduction was observed in Si_{10} PCL-PGP containing composites. The higher release rate of the phosphate species led to an acidic medium through the formation of phosphoric acid [6, 28]. However, by substituting Si_{10} with Fe_{10} PGP, the rate of release of phosphate species and pH change was reduced.

In Fe_{10} containing composites, glass particles were still present at day 56 in deionised water. Therefore, in composites containing blends of glass formulations, pores, formed by rapid dissolution of the Si_{10} PGP and remnants Fe_{10} PGP were observed. By controlling the initial glass particle size and through their dissolution, defined pore sizes could be created. An advantage of such a structure, *in vivo*, would be that if the pores were designed to be interconnected, an increase in the potential for nutrient and oxygen perfusion and cell migration and growth would be achieved, while favourable ionic species would still being released. In addition, the newly formed porous composite maintains its mechanical properties for longer time periods.

Flexural mechanical analyses were performed to measure the mechanical properties of the various composites, initially and post ageing in PBS. Initially, there was no significant change in flexural strength in the composites relative to neat PCL except for the Si_{10} containing PCL-PGP composites. On the other hand, the Young's modulus of PCL-PGP composites was significantly higher than the modulus of PCL, which increased with an increase in Si_{10} PGP. Ahmed *et al* [32] studied the flexural properties of a binary PG fibres ($50P_2O_5$-$50CaO$) reinforced PCL and showed that there was no significant change in strength. However, the modulus displayed a five-fold increase from 0.5 to 2.4 GPa at 18 vol%. Previously Georgiou *et al* [6] demonstrated a significant increase in the storage modulus of PGP incorporated polylactic acid composites at 20 wt%. In this study, the increase in modulus was also accompanied by a significant decrease in the strain at maximum stress. These effects indicated a higher level of particle-matrix interaction that result in more stress transfer between the particles and the matrix, thus leading to a higher modulus and reduced matrix ductility at the vicinity of the particles with lower strain at maximum stress. Given that all inclusions were at 40 vol%, it was hypothesised that an interfacial interaction between PGP and PCL occurred during their processing, which increased with an increase in Si_{10} content. It has been previously reported that silicate based glasses [29] can cause polyester chain scission (reduction in M_w) when processed at elevated temperatures. In this study, PCL M_w determination revealed similar results, where there was dramatic decrease in M_w with an increase in Si_{10} PGP content, which was not demonstrated with Fe_{10} PGP. In turn, this affected the mechanical properties of the as prepared composites [29, 33, 34]. The ageing of the composites showed no significant change in PCL M_w, thus confirming that the changes were due to the glass particle dissolution.

The ageing of Si_{10} PCL-PGP in PBS caused a dramatic decrease in its mechanical properties. The rate of decrease was considerably less in composites of increasing Fe_{10} content. This was in line with the weight loss behaviour and the potential for pore generation due to Si_{10} dissolution. Since the solubility of Fe_{10} was relatively low, the material can retain its mechanical properties for longer periods of time by increasing the Fe_{10} content. These differences support the hypothesis that the mechanical property retention characteristics of these composites may be controlled by altering the PGP blends.

ATR-FTIR on the composites revealed an increase of the fractional absorbance change at 1728 cm^{-1}, *i.e.* a decrease in the absorbance of the C=O bond peak, in the presence of the Si_{10} while no such reduction occurred in neat PCL and PCL-PGP 5 (supplementary data). By increasing the amount of Si_{10} contents in the composite, the extent of these changes was higher and occurred at a faster rate. Moreover, formation of a carboxylate peak (1634 cm^{-1}) became evident in the presence of Si_{10} and did not occur for neat PCL and Fe_{10} dominant composites. This and accompanying changes in the ester data suggest that Si containing glasses react with the ester bonds due to the high processing temperatures involved. This reaction breaks down the ester bonds and leads to the formation of carboxylate by-products which result in the formation of lower molecular weight polymer as has been proposed by Blaker *et al.* [29] for silicate based glasses (e.g. Bioglass®).

Weight loss in SBF displayed a similar trend to that in DW; however, at a lower extent due to the presence of ions in SBF. The pH of SBF was reduced to below pH 4, which was controlled by Fe_{10} content (i.e. the higher the Fe_{10} content the lower the dissolution). SBF conditioning resulted in the formation of brushite on the surface of PCL-PGP 3 at day 28. According to the calcium phosphate phase diagram, several calcium phosphates can form with a well defined solubility among which only one can be most stable [35]. Therefore, in true thermodynamic equilibrium, phases with greater solubility exist in metastable equilibrium. Ultimately, the metastable phosphates will transform to stable compounds via intermediate phases. The composition of the solution is fixed at a singular point where the isotherms for two phosphates cross over and the position at which the solubility of the salts interchange. The singular point for brushite ($CaHPO_4.2H_2O$) and HA ($Ca_{10}(PO_4)_6(OH)_2$) is at a pH of 4.3 at 25 °C [35]. Brushite and HA are stable below and above this pH, respectively [35]. Franks *et al* [18] confirmed that the formation of a brushite precipitate is an indication of the bioactivity of phosphate-based glasses, where brushite is a possible precursor to the formation of apatite [18, 36]. Abou Neel *et al* [37] showed that in the case of PG based on $50P_2O_5$-(15-20)Na_2O-30CaO-(0-5mol%)TiO_2, no evidence of apatite formation was observed at day 14 in SBF despite favourable cell response and gene up-regulation. In this study, evidence of brushite formation was only observed at day 28 for mixed glass formulations indicating that longer times were required for calcium phosphate precipitate formation on the surface of these glasses as in the case of PCL-PG3. PCL-PGP 1 showed no precipitation, which was probably due to the very rapid dissolution rate of Si_{10} where there was a dramatic increase in the amount and rate of PO_4^{3-} ion release in the first 24 hours. In contrast, PCL-PGP 5 rate of dissolution was very slow. Therefore, the use of mixed glass formulations could control the amount and rate of ion release where there is a significant effect on the potential for calcium phosphate precipitation. The rate of resorption and associated ion release of bone graft substitutes has been highlighted as an important factor in their successful application [38]. Future studies will focus on the biological properties of the composites of mixed reinforcements through their interactions with osteoblastic cells.

5. Conclusions

The effect of mixed phosphate glass fillers with different formulations on the properties of PCL composites was investigated. Whilst no weight loss was observed for PCL alone over the course of this study, incorporating high and low solubility phosphate-based glass formulations into a composite resulted in a wide range of weight loss rates, from very high for 40%Si_{10}-0%Fe_{10} to very low for 0%Si_{10}-40%Fe_{10}. Blends of both Si_{10} and Fe_{10} showed intermediate weight loss rates. As a consequence, Si_{10} PGP led to the formation of porosities while Fe_{10} PGP remained in the composites for longer time periods. A correlation was observed between the amount of Si_{10}

content and ions released, where the release of PO_4^{3-}, Ca^{2+}, Fe^{3+}, and Si^{4+} ions increased significantly with Si_{10} content.

Composite mechanical properties were also affected by glass formulation, both initially and as a function of time in PBS. An increase in Si_{10} content, led to a reaction between PG and PCL matrix when processed at high temperature, causing chain scission and a concomitant reduction in molecular weight, which significantly reduced the mechanical properties of the composites. Reinforcements of mixed glass formulations resulted in a lower decrease rate of mechanical properties through ageing in PBS. At day 28 in SBF, brushite formation was indicated on the surfaces of the composites of mixed glass formulations. Therefore, incorporation of mixed phosphate glass fillers within degradable polymer matrices may be effective in tailoring the properties required for bone repair and regeneration.

References

[1] Boccaccini AR, Maquet V. Bioresorbable and bioactive polymer/Bioglass® composites with tailored pore structure for tissue engineering applications. Compos Sci Technol 2003;63:2417–2429.

[2] Ramakrishna S, Mayer J, Wintermantel E, Leong KW. Biomedical applications of polymer composite materials: a review. Compos Sci Technol 2001;61:1189–224.

[3] Rich J, Jaakkola T, Tirri T, Naärhi T, Yli-Urpo A, Seppälä J. In vitro evaluation of poly(epsilon-caprolactone-co-DL-lactide)/bioactive glass composites. Biomaterials 2002;23: 2143–2150.

[4] Ma PX, Zhang R, Xiao G, Franceschi R. Engineering new bone tissue in vitro on highly porous poly(α-hydroxy acids)/hydroxyapatite composite scaffolds. J Biomed Mater Res 2001;54:284–293.

[5] Rizzi S, Heath D, Coombes A, Bock N, Textor M, Downes S. Biodegradable polymer/hydroxyapatite composites: surface analysis and initial attachment of human osteoblasts. J Biomed Mater Res 2001;55:475–486.

[6] Georgiou G, Mathieu L, Pioletti DP, Bourban PE, Manson JAE, Knowles JC, Nazhat SN. Polylactid acid-phosphate glass composite foams as scaffolds for bone tissue engineering. J of Biomed Mater Res Part B: Applied Biomaterials 2006; 322-331.

[7] Andriano KP, Daniels AU, Smutz WP, Wyatt RWB, Heller J. Preliminary biocompatibility screening of several biodegradable phosphate fiber reinforced polymers. J Appl Biomater 1993;4:1–12.

[8] Navaro M, Ginebra MP, Planell JA, Barrias CC, Barbosa MA. In vitro behavior of a novel bioresorbable composite material based on PLA and a soluble CaP glass. Acta Biomaterialia 2005;1:411-419.

[9] Charles-Harris M, Del Valle S, Hentges E, Bleuet P, Lacroixa D, Planell JA. Mechanical and structural characterisation of completely degradable polylactic acid/calcium phosphate glass scaffold. Biomaterials 2007;28:4429-4438.

[10] Nazhat SN, Kellomaki M, Tormala P, Tanner KE, Bonfield W. Dynamic mechanical characterization of biodegradable composites of hydroxyapatite and polylactides. J Biomed Mater Res 2001;58:335–343.

[11] Bleach NC, Nazhat SN, Tanner KE, Kellomäki M, Törmälä P. Effect of filler content on mechanical and dynamic mechanical properties of particulate biphasic calcium phosphate polylactide composites. Biomaterials 2002;23:1579–1585.

[12] Dupraz AMP, de Wijn JR, vd Meer SAT, de Groot K. Characterization of silane-treated hydroxyapatite powders for use as filler in biodegradable composites. J Biomed Mater Res 1996; 30:231–238.

[13] Klein CPAT, Driessen AA, Degroot K, Vandenhooff A. Biodegradation behavior of various calcium-phosphate materials in bone tissue. J Biomed Mater Res 1983;17:769 –784.

[14] Knowles JC. Phosphate based glasses for biomedical applications, J Mater Chem 2003, 13:2395–2401.

[15] Abou Neel EA, Pickup DM, Valappil SP, Newport RJ, Knowles JC. Bioactive functional materials: a perspective on phosphate-based glasses, J Mater Chem 2009,19:690-701.

[16] Patel A, Knowles JC. Investigation of silica-iron-phosphate glasses for tissue engineering. J Mater Sci: Mater Med 2006;17:937-944.

[17] Gao H, Tan T, Wang D. Effect of composition on the release kinetics of phosphate controlled release glasses in aqueous medium. J Controlled Release 2004;96:21-28.

[18] Franks K, Abrahams I, Knowles JC. Development of soluble glasses for biomedical use part 1: in vitro solubility measurement. J Mater Sci: Mater Med 2000;11:609-614.

[19] Bunker BC, Arnoled GW, Wilder JA. Phosphate glass dissolution in Aqueous solutions, Journal of Non-Crystalline Solids 1984;64:291-316.

[20] Abou Neel EA, Knowles JC. Physical and biocompatibility studies of novel titanium dioxide doped phosphate-based glasses for bone tissue engineering applications. J Mater Sci: Mater Med 2008;19:377-386.

[21] Ahmed I, Parson AJ, Nazhat SN, Guerry P, Smith ME, Knowles JC and Rudd CD. Comparison of phosphate-based glasses in the range $50P_2O_5$-(50-x)CaO-xNa2O prepared using different precursors. J Glass Sci Technol A 2008; 49:63-72.

[22] Ahmed I, Lewis M, Olsen I, Knowles JC. Phosphate glasses for tissue engineering: part 1. Processing and characterization of a ternary-based P_2O_5-CaO-Na_2O glass system. Biomaterials 2004;25:491-499.

[23] Ahmed I, Lewis M, Olsen I, Knowles JC. Phosphate glasses for tissue engineering: part 2. Processing and characterization of a ternary-based P_2O_5-CaO-Na_2O glass fibre system. Biomaterials 2004;25:501-507.

[24] Gough JE, Christian P, Scotchford CA, Rudd CD, Jones IA. Synthesis, degradation, and *in vitro* cell response of sodium phosphate glasses for craniofacial bone repair. J Biomed Mater Res 2002;59:481-489.

[25] Gough JE, Christian P, Scotchford CA, Jones IA. Long-term craniofacial osteoblast culture on a sodium phosphate and a calcium/sodium phosphate glass. J Biomed Mater Res 2003;66A: 233-240.

[26] Salih V, Franks K, James M, Hastings GW, Knowles JC. Development of soluble glass for biomedical use. Part 2: the biological response of human osteoblast cell lines to phosphate-based soluble glasses. J Mater Sci: Mater Med 2000;11:615-620.

[27] Ahmed I, Collins CA, Lewis M, Olsen I, Knowles JC. Processing, characterization and biocompatibility of iron-phosphate glass fibres for tissue engineering. Biomaterials 2004; 25:3223-3232.

[28] Abou Neel EA, Ahmed I, Blaker JJ, Bismark A, Boccaccini AR, Lewis MP, Nazhat SN, Knowles JC. Effect of iron on the surface, degradation and ion release properties of phosphate-based glass fibres. Acta Biomaterialia 2005;1:553-563.

[29] Blaker JJ, Bismarck A, Boccaccini AR, Young AM, Nazhat SN. Premature degradation of poly(α-hydroxyesters) during thermal processing of Bioglass® containing composites, Acta Biomaterialia, In press.

[30] Kokubo T, Takadama H. How useful is SBF in predicting in vivo bone bioactivity? Biomaterials 2006;27:2907-2915.

[31] Ahmed I, Lewis MP, Nazhat SN, and Knowles JC. Quantification of Anion and Cation Release from a Range of Ternary Phosphate-based Glasses with Fixed 45mol% P_2O_5. Journal of Biomaterials Applications 2005;20:65-80.

[32] Ahmed I, Parsons AJ., Palmer G, Knowles JC, Walker GS, Rudd CD. Weight loss, ion release and initial mechanical properties of a binary calcium phosphate glass fibre/PCL composite. Acta Biomaterialia 2008;4:1307–1314.

[33] Niemelä T, Niiranen H, Kellomäki M, Törmälä. Self-reinforced composites of bioabsorbable polymer and bioactive glass with different bioactive glass contents. Part I: Initial mechanical properties and bioactivity. Acta Biomateriala 2005;1:235-242.

[34] Niiranen H, Pyhältö T, Rokkanen P, Kellomäki M, Törmälä P. *In vitro* and *in vivo* behaviour of self-reinforced bioabsorbable polymer and self-reinforced bioabsorbable polymer/bioactive glass composites. J Biomed Mater Res 2004;69A:699-708.

[35] Williams RAD, Elliott JC. Basic and applied dental biochemistry. Churchill livingstone, Edinburgh, London, and New York, 1989.

[36] Johnson MSA, Nancollas GH. The role of brushite and octacalcium phosphate in apatite formation. Critical Reviews in Oral Biology and Medicine 1992;3:61-82.

[37] Abou Neel EA, Mizoguchi T, Michio I, Bitar M, Salih V, Knowles JC. *In vitro* bioactivity and gene expression by cells cultured on titanium dioxide doped phosphate-based glasses. Biomaterials 2007;28:2967-2977.

[38] Bohner M. Silicon-substituted calcium phosphates – A critical view. Biomaterials 2009;30:6403-6406.

List of Tables

Table 1 Glass formulations and codes

Table 2 Composites compositions and codes

Table 3 Weight loss and residual glass of the samples in the final dry weight of the specimens after 56 days. There was no residual glass in the composites containing high amount of Si_{10} glass and low amount of Fe_{10}. The percentage of remaining glass increased with an increase in the amount of Fe_{10}

Figure captions

Figure 1 Ageing of PCL and PCL-PGP composites in DW incubated up to 56 days at 37 °C. (a) PO_4^{3-} (b) Ca^{2+} (c) Si^{4+} and (d) Fe^{3+} ion release from PCL-PGP composites. Anion and cation release increased with increasing Si_{10} content. (e) Weight loss measurements, and (f) pH changes. An initial decrease was observed for composites containing Si_{10} which increased with Si_{10} content in the composites.

Figure 2 SEM micrographs of (a) as processed cryo-fractured PCL-PGP 3 composite, (b) PCL-PGP 3 at day 56 immersion in DW, and (c) PCL-PGP 1 at day 56 in deionised water. As processed composites showed well dispersed and attached PGP on PCL matrix. While all Si_{10} PGPs underwent dissolution in PCL-PGP 1 at day 56, there were residual Fe_{10} PGPs in the composites.

Figure 3 Mechanical property changes in PBS (a) Weight loss of neat PCL and PCL-PGP composites at days 7 and 28 ageing in PBS, wet, and at day 28, dry. As processed and post PBS conditioning flexural mechanical properties of PCL and PCL-PGP composites: (b) flexural strength, (c) Young's modulus, and (d) strain at maximum stress. Initial flexural strength remained almost constant via the addition of PGP except for PCL-PGP 1 where a statistically significant ($P<0.05$) decrease was observed. By increasing Si_{10} content, Young's modulus increased, and strain at maximum stress decreased significantly. After ageing in PBS, the decrease in mechanical properties was considerably higher for high Si_{10} dominant composites compared to high Fe_{10} dominant composites.

Figure 4 (a) Molecular weight, and (b) polydisersity index of neat PCL and PCL in the composites, as processed and post conditioning in DW. There is no difference in the molecular weight of PCL M_w in the Fe_{10} containing composites when compared to the neat PCL. However, there was a decrease in PCL M_w with increasing Si_{10} content. There was no change in PCL M_w in all systems as a consequence of conditioning in DW. Similarly the polydispersity index remains almost constant.

Figure 5 FTIR analyses. (a) The fractional absorbance change of carbonyl peak (1728 cm^{-1}) for PCL and PCL-PGP composites. There was a considerable increase of ϕ_{1728} for PCL-PGP 3 and 5 during thermal treatment at 100°C. (b) FTIR spectra of PCL-PGP 1 before and after the thermal treatment. There was a reduction in the absorbance of C=O peak at 1728 cm^{-1}, and a concomitant appearance of a carboxylate peak at 1634 cm^{-1}. (c) Comparison of the carboxylate peak formation for PCL and PCL-PGP composites. The carboxylate peak became more apparent as the Si_{10} content in the composites increased as shown in PCL-PGP 3 and 1. Neat PCL and PCL-PGP 5 displayed no carboxylate peaks.

Figure 6 (a) Weight loss of PCL and PCL-PGP composites through conditioning in SBF. A significant weight loss was observed for high Si_{10} containing composites. (b) pH changes obtained for PCL and PCL-PGP composites up to 1 week in SBF. While there was a prompt reduction in the pH to below 4, the required time for this reduction increased with Fe_{10} content.

Figure 7 Analyses of the precipitates formed on PCL-PGP composites through conditioning in SBF. Images at days 7, 14, and 28, SEM micrographs and EDS spectra at day 28 of (a) PCL-PGP 5, (b) PCL-PGP 3, and (c) PCL-PGP 1. XRD patterns of (d) PCL-PGP 3 as made, and at days 14 and 28 in SBF, and e) PCL-PGP 5, 3, and 1 at day 28 in SBF.

Figure 1

Click here to download high resolution image

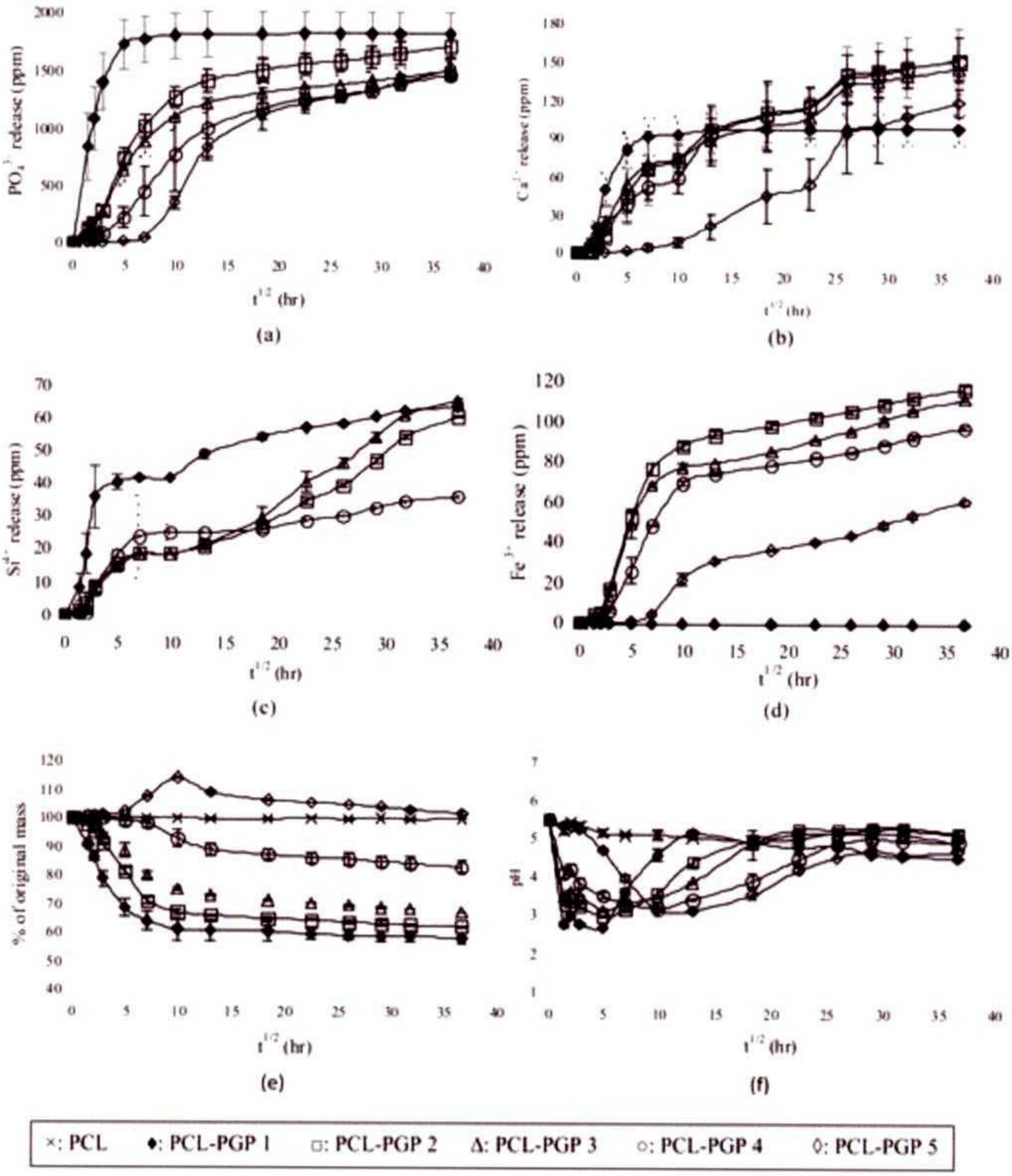

(a) (b) (c) (d) (e) (f)

Figure 2

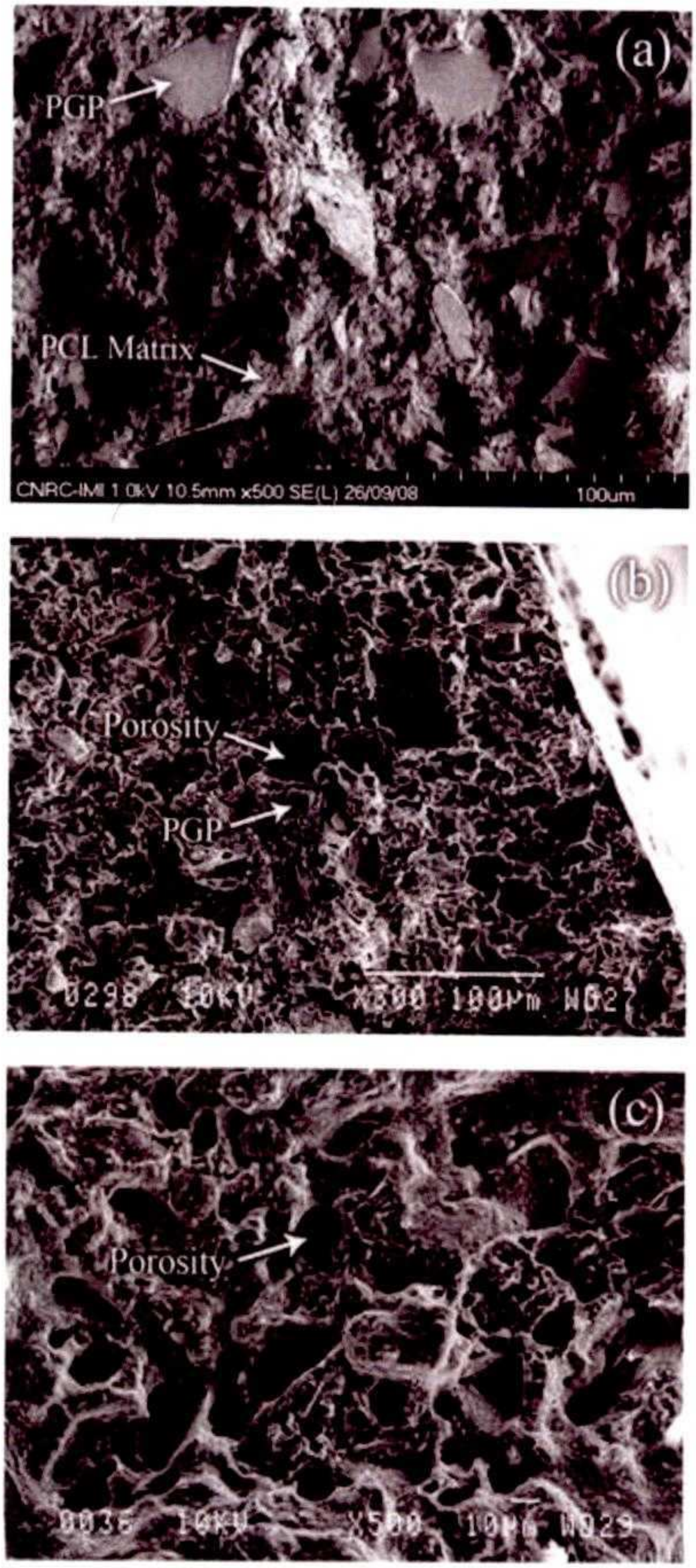
(a)
PGP
PCL Matrix
CNRC-IMI 1.0kV 10.5mm x500 SE(L) 26/09/08
100um
(b)
Porosity
PGP
0298 10KV X300 100µm WD27
(c)
Porosity
0036 10KV X500 10µm WD29

Figure 3

Click here to download high resolution image

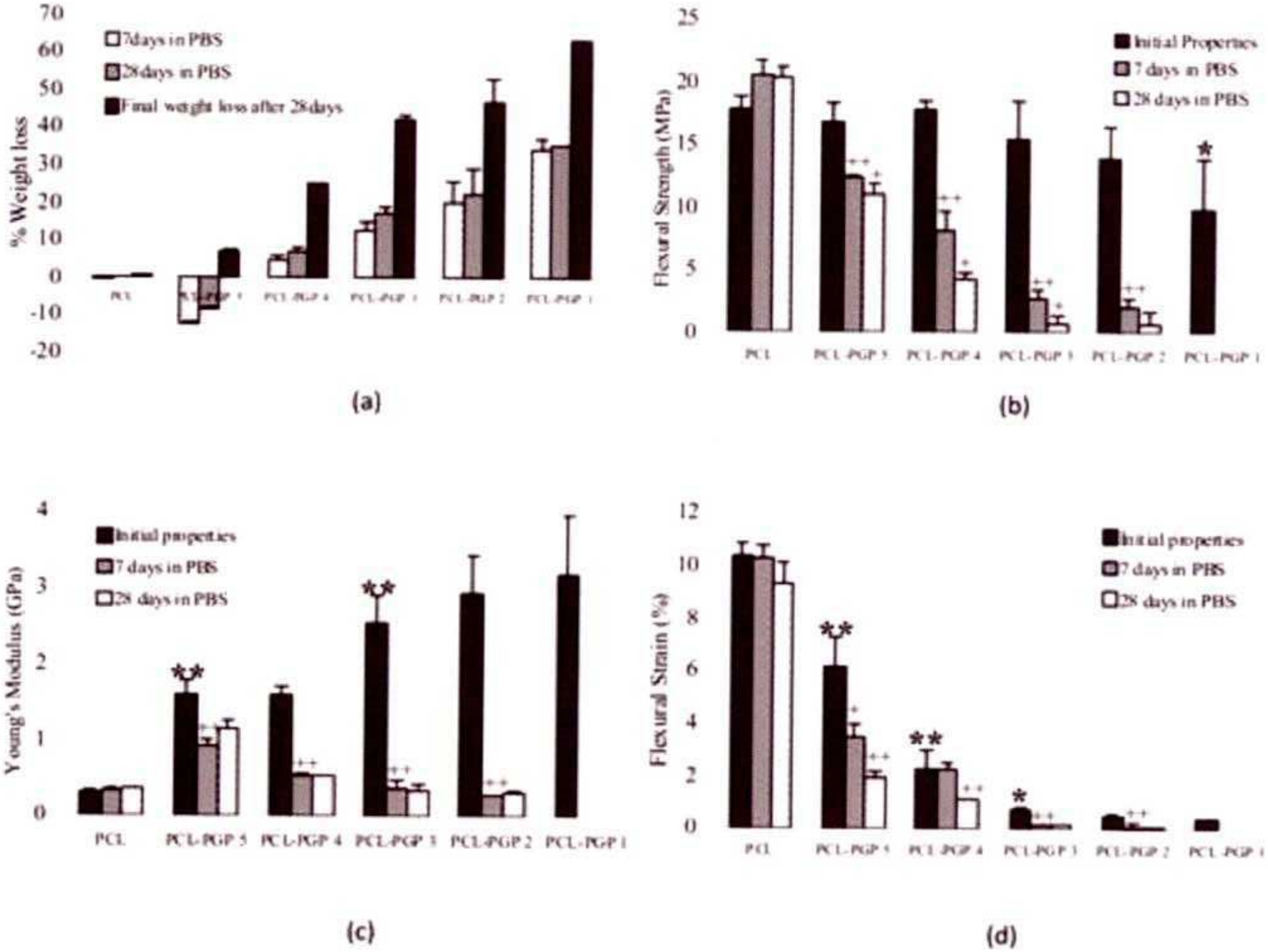

*: Statistically significant difference compared to previous material at the same time point

**: Very statistically significant difference compared to previous material at the same time point

+: Statistically significant difference compared to previous time point for the same material

++: Very statistically significant difference compared to previous time point for the same material

Figure 4

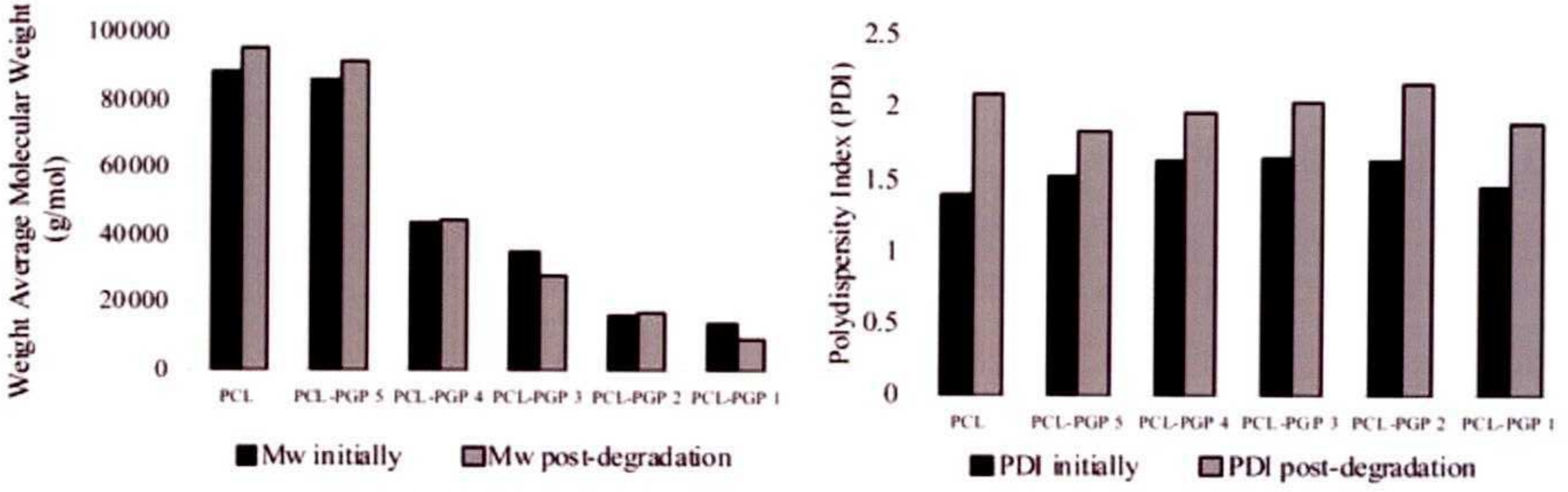
Weight Average Molecular Weight (g/mol)
100000
80000
60000
40000
20000
0
PCL
PCL-PGP 5
PCL-PGP 4
PCL-PGP 3
PCL-PGP 2
PCL-PGP 1
■ Mw initially
▨ Mw post-degradation
Polydispersity Index (PDI)
2.5
2
1.5
1
0.5
0
PCL
PCL-PGP 5
PCL-PGP 4
PCL-PGP 3
PCL-PGP 2
PCL-PGP 1
■ PDI initially
▨ PDI post-degradation

(a)

(b)

Figure 5

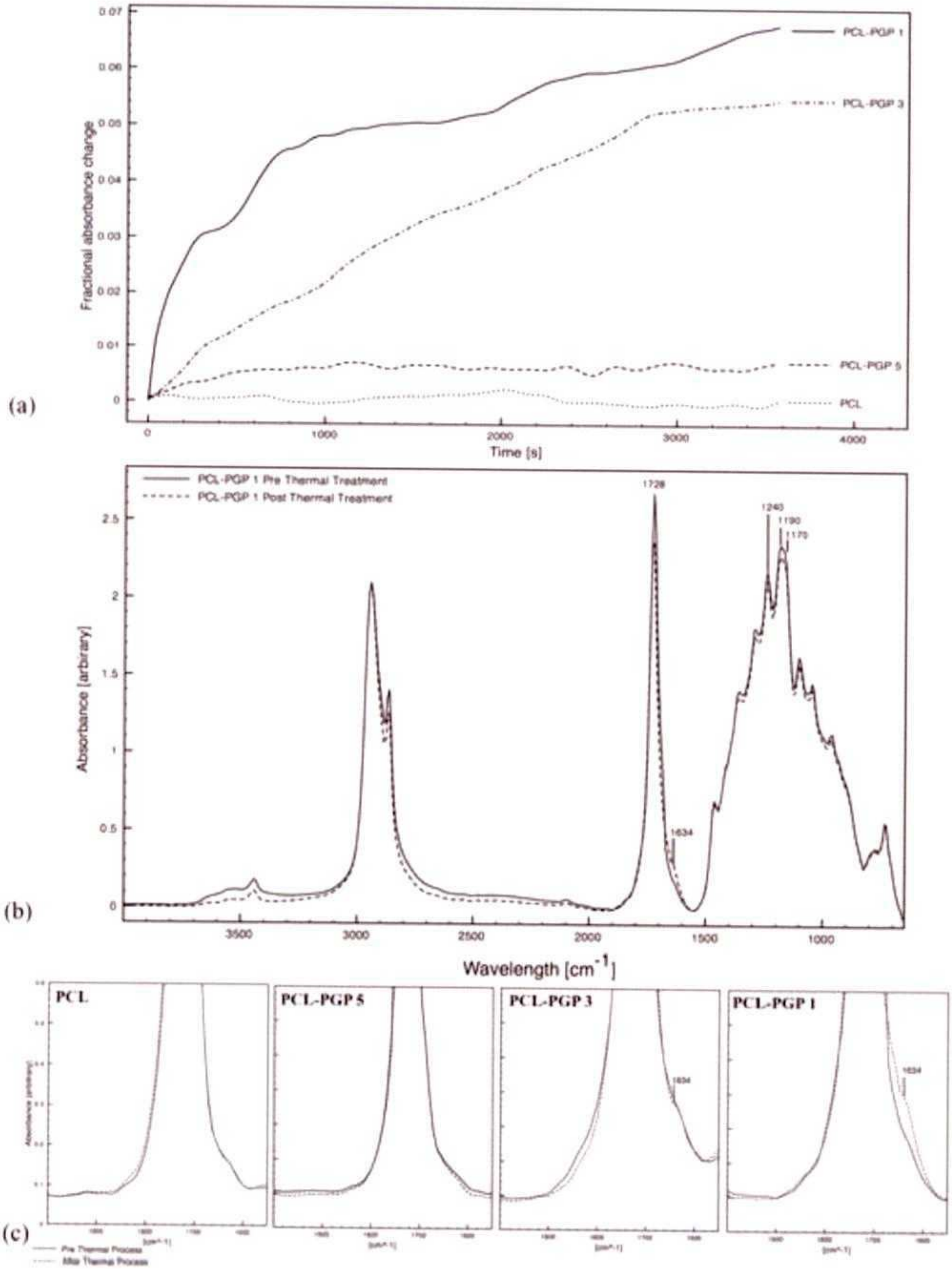
(a)
Fractional absorbance change
0.07
0.06
0.05
0.04
0.03
0.02
0.01
0
0
1000
2000
3000
4000
Time [s]
PCL-PGP 1
PCL-PGP 3
PCL-PGP 5
PCL
(b)
PCL-PGP 1 Pre Thermal Treatment
PCL-PGP 1 Post Thermal Treatment
Absorbance [arbitrary]
2.5
2
1.5
1
0.5
0
1728
1240
1190
1170
1634
3500
3000
2500
2000
1500
1000
Wavelength [cm^{-1}]
(c)
PCL
PCL-PGP 5
PCL-PGP 3
PCL-PGP 1
1634
1634
Absorbance [arbitrary]
[cm^-1]
Pre Thermal Process
After Thermal Process

Figure 6

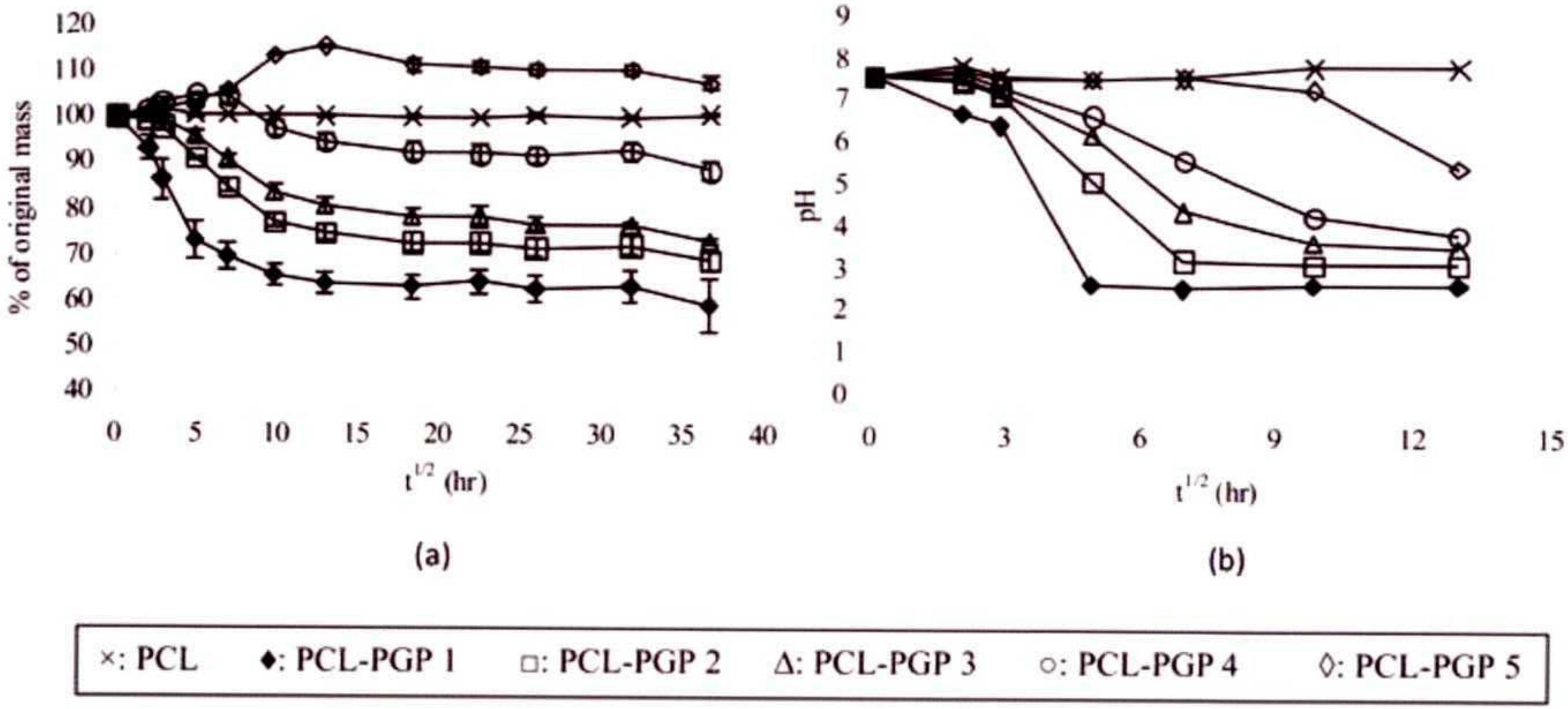
% of original mass
120
110
100
90
80
70
60
50
40
0
5
10
15
20
25
30
35
40
t^1/2 (hr)
pH
9
8
7
6
5
4
3
2
1
0
0
3
6
9
12
15
t^1/2 (hr)
×: PCL
♦: PCL-PGP 1
□: PCL-PGP 2
Δ: PCL-PGP 3
○: PCL-PGP 4
◊: PCL-PGP 5

(a)

(b)

Figure 7

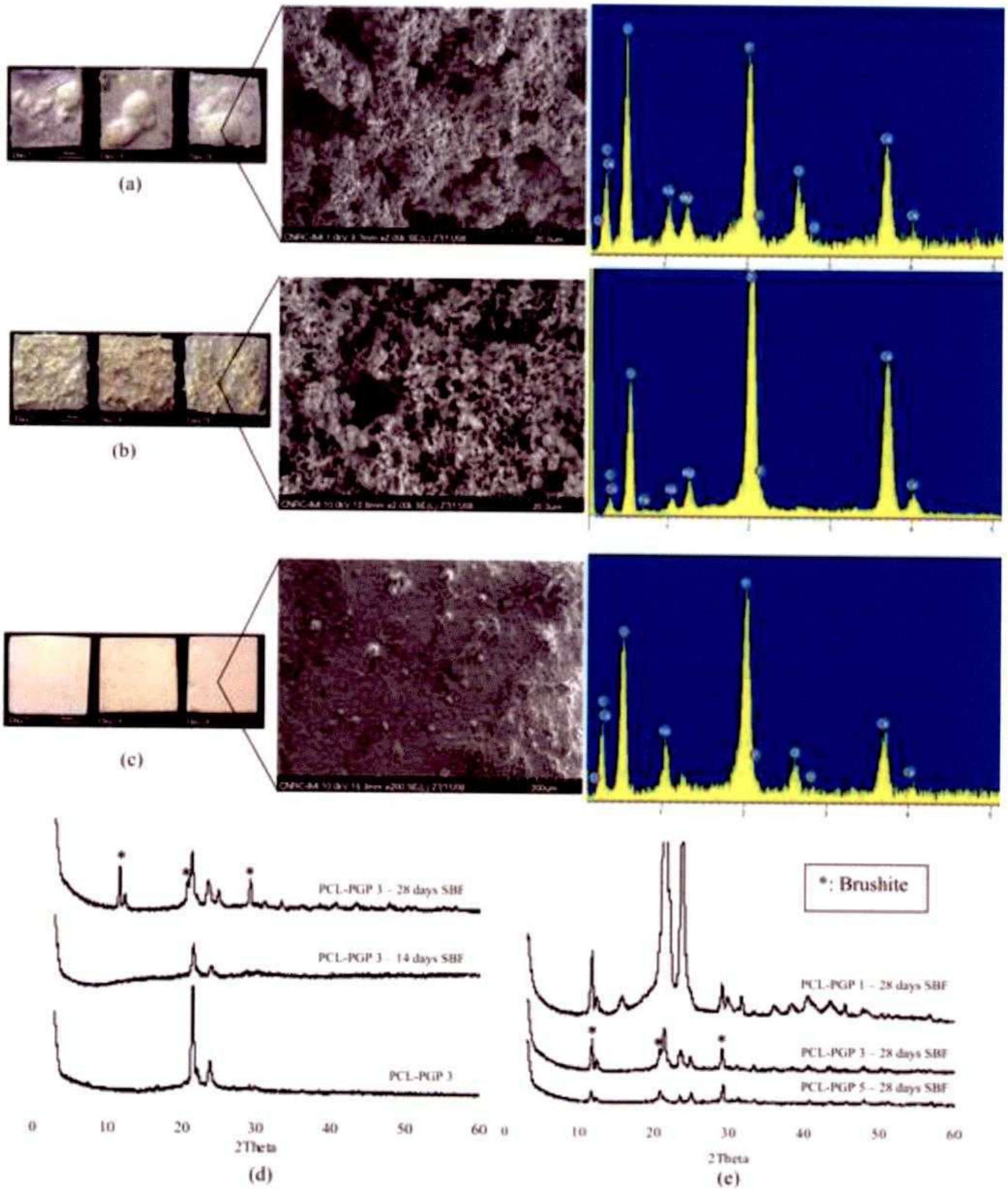
(a)
(b)
(c)
*
PCL-PGP 3 - 28 days SBF
PCL-PGP 3 - 14 days SBF
PCL-PGP 3
0
10
20
30
40
50
60
2Theta
(d)
*: Brushite
PCL-PGP 1 - 28 days SBF
PCL-PGP 3 - 28 days SBF
PCL-PGP 5 - 28 days SBF
0
10
20
30
40
50
60
2 Theta
(e)

Table 1

Glass Code	Components (Mol. %)			
	P_2O_5	CaO	SiO_2	Fe_2O_3
Si_{10}	50	40	10	-
Fe_{10}	50	40	-	10

Table 2

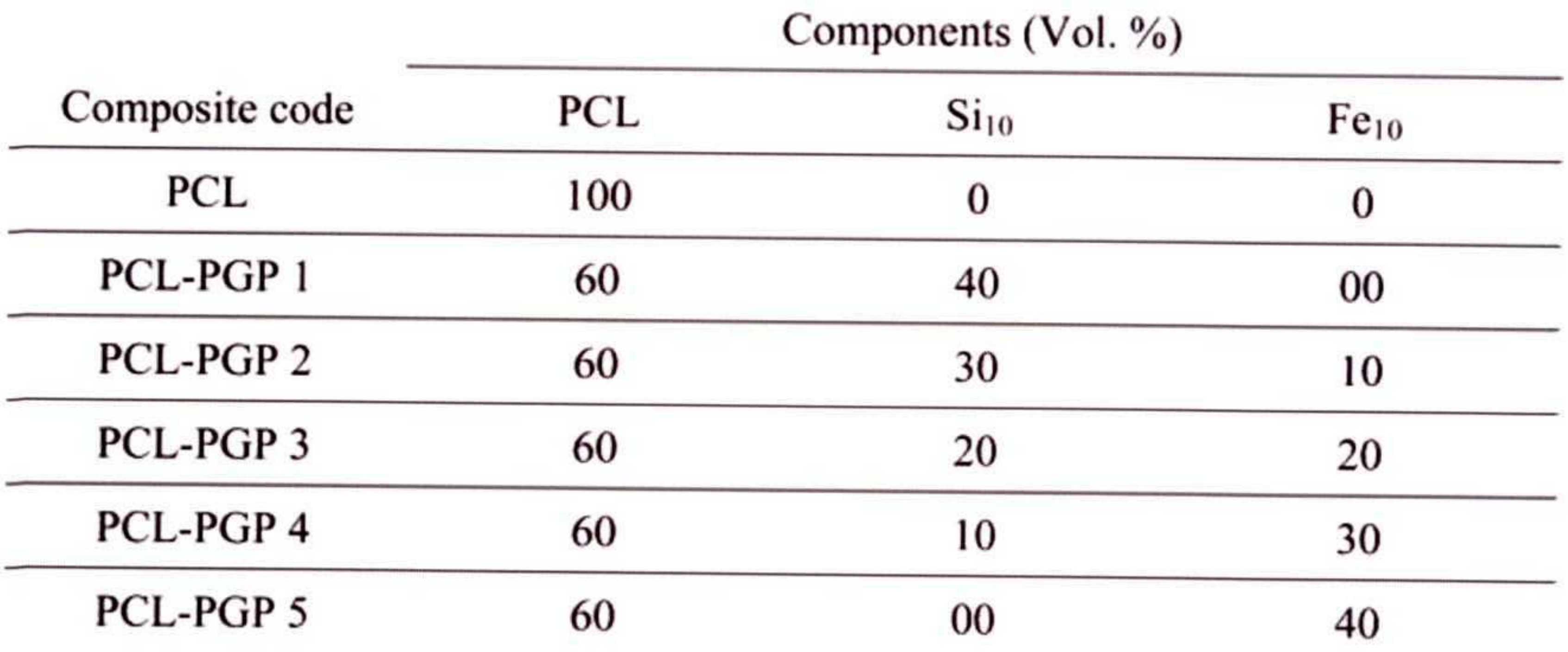

Composite code	Components (Vol. %)		
	PCL	Si_{10}	Fe_{10}
PCL	100	0	0
PCL-PGP 1	60	40	00
PCL-PGP 2	60	30	10
PCL-PGP 3	60	20	20
PCL-PGP 4	60	10	30
PCL-PGP 5	60	00	40

Table 3

Material	% of original mass	Remaining Glass (%)
PCL	99.39 ± 0.06	-
PCL-PGP 1	34.91 ± 3.02	0
PCL-PGP 2	40.25 ± 0.12	0
PCL-PGP 3	46.53 ± 1.12	12
PCL-PGP 4	65.33 ± 2.82	44
PCL-PGP 5	81.66 ± 1.07	67

Supplementary Material